Journal of Bacteriology

Nonredundant Roles for Cytochrome c_2 and Two High-Potential Iron-Sulfur Proteins in the Photoferrotroph Rhodopseudomonas palustris TIE-1

Lina J. Bird, Ivo H. Saraiva, Shannon Park, Eduardo O. Calçada, Carlos A. Salgueiro, Wolfgang Nitschke, Ricardo O. Louro and Dianne K. Newman

J. Bacteriol. **2014, 196(4):850. DOI: 10.1128/JB.00843-13. Published Ahead of Print 6 December 2013.**

JB Journals.ASM.org

Nonredundant Roles for Cytochrome c_2 and Two High-Potential Iron-Sulfur Proteins in the Photoferrotroph *Rhodopseudomonas palustris* TIE-1

Lina J. Bird,[a,b] Ivo H. Saraiva,[c] Shannon Park,[b] Eduardo O. Calçada,[d] Carlos A. Salgueiro,[d] Wolfgang Nitschke,[e] Ricardo O. Louro,[c] Dianne K. Newman[b]

Department of Biology, Massachusetts Institute of Technology, Cambridge, Massachusetts, USA[a]; Divisions of Biology and Geological and Planetary Sciences, Howard Hughes Medical Institute at the California Institute of Technology, Pasadena, California, USA[b]; Instituto de Tecnologia Química e Biológica, Universidade Nova de Lisboa, Oeiras, Portugal[c]; Requimte, CQFB, Departamento de Química, Faculdade de Ciências e Tecnologia da Universidade Nova de Lisboa, Monte da Caparica, Portugal[d]; Laboratoire de Bioénergétique et Ingénierie des Protéines (UMR7281), CNRS/AMU, FR3479, Marseille, France[e]

The purple bacterium *Rhodopseudomonas palustris* TIE-1 expresses multiple small high-potential redox proteins during photoautotrophic growth, including two high-potential iron-sulfur proteins (HiPIPs) (PioC and Rpal_4085) and a cytochrome c_2. We evaluated the role of these proteins in TIE-1 through genetic, physiological, and biochemical analyses. Deleting the gene encoding cytochrome c_2 resulted in a loss of photosynthetic ability by TIE-1, indicating that this protein cannot be replaced by either HiPIP in cyclic electron flow. PioC was previously implicated in photoferrotrophy, an unusual form of photosynthesis in which reducing power is provided through ferrous iron oxidation. Using cyclic voltammetry (CV), electron paramagnetic resonance (EPR) spectroscopy, and flash-induced spectrometry, we show that PioC has a midpoint potential of 450 mV, contains all the typical features of a HiPIP, and can reduce the reaction centers of membrane suspensions in a light-dependent manner at a much lower rate than cytochrome c_2. These data support the hypothesis that PioC linearly transfers electrons from iron, while cytochrome c_2 is required for cyclic electron flow. Rpal_4085, despite having spectroscopic characteristics and a reduction potential similar to those of PioC, is unable to reduce the reaction center. Rpal_4085 is upregulated by the divalent metals Fe(II), Ni(II), and Co(II), suggesting that it might play a role in sensing or oxidizing metals in the periplasm. Taken together, our results suggest that these three small electron transfer proteins perform different functions in the cell.

Soluble *c*-type cytochromes and high-potential iron-sulfur proteins (HiPIPs) are small redox-active proteins that have long been known to act as electron donors to the reaction centers of anoxygenic phototrophs (1). The HiPIPs contain a [4Fe-4S] cubane cluster coordinated by four cysteine residues and have reduction potentials that range from 50 to 500 mV (2). They occur in a wide variety of organisms, both phototrophic and nonphototrophic. The small soluble cytochromes used in photosynthesis (such as cytochrome c_2) contain a single *c*-type heme and have reduction potentials ranging from 150 to 380 mV (3).

A survey of photosynthetic bacteria (4) showed that many contain either a HiPIP or a small cytochrome *c*, leading to the conclusion that either protein could serve as an electron shuttle between the cytochrome bc_1 complex and the reaction center during photosynthetic energy generation. Many bacteria contain both small cytochromes and HiPIPs and sometimes contain multiple copies of each, a redundancy that has yet to be fully explained. Biophysical studies have shown that, in at least some of the organisms containing a HiPIP and a small cytochrome, both are capable of reducing the reaction center (5–8). Under a given condition, a single protein (either the HiPIP or the cytochrome) generally appears to be the dominant electron donor (6). However, mutant studies have shown that in *Rubrivivax gelatinosus*, three small *c*-type cytochromes can partially substitute when the dominant donor to the reaction center, a HiPIP, is deleted (9).

In the phototrophs studied so far, those in which the dominant electron donor is a HiPIP also contain a tetraheme cytochrome bound to the reaction center (4). The tetraheme cytochrome reduces the bacteriochlorophyll and is in turn reduced by a soluble donor. All biophysical studies of photosynthetic HiPIPs in wild-type bacteria show that the HiPIP interacts with the tetraheme cytochrome rather than directly with the reaction center (5–7, 10, 11). However, one study in a *Rubrivivax gelatinosus* mutant lacking the tetraheme cytochrome showed that a HiPIP can donate electrons to the reaction center, though at a reduced rate (12). In addition, there are a number of photosynthetic bacteria that contain HiPIPs in their genome but lack the tetraheme cytochrome. *Rhodopseudomonas palustris* is an example of the last category. It is a purple nonsulfur bacterium that has both types of electron shuttles: its genome encodes two HiPIPS and two cytochromes c_2 but no tetraheme cytochrome. Precisely how bacteria like *R. palustris* utilize their HiPIPs is an open question.

Our interest in this problem originated from study of the electron transfer pathway involved in phototrophic growth on ferrous iron [Fe(II)] (photoferrotrophy). Photoferrotrophy was first described in 1993, and *R. palustris* TIE-1 was the first genetically

Received 2 August 2013 Accepted 28 November 2013
Published ahead of print 6 December 2013
Address correspondence to Ricardo O. Louro, louro@itqb.unl.pt, or Dianne K. Newman, dkn@caltech.edu.
L.J.B. and I.H.S. are co-first authors.
Supplemental material for this article may be found at http://dx.doi.org/10.1128/JB.00843-13.

doi:10.1128/JB.00843-13

tractable photoferrotroph to be isolated (13). Following its isolation, the *pio* operon was shown to be required for photosynthetic iron oxidation (14). Three genes comprise this operon: *pioA* (encoding a decaheme *c*-type cytochrome), *pioB* (encoding a putative outer membrane porin), and *pioC* (encoding a HiPIP) (14). Interestingly, although the Δ*pioC* mutant could not grow on iron, it was still able to oxidize Fe(II), though at a lower rate than the wild-type strain. We hypothesized that the residual oxidation activity was provided by the second HiPIP, Rpal_4085. The Δ*pioC* mutant was also not impaired for other forms of photosynthetic growth. Although genetic studies indicated that PioC has a specialized role in Fe(II) oxidation, questions about the function and mechanism of the HiPIPs in *R. palustris* TIE-1 remained. Do the HiPIPs donate to the reaction center, even without a tetraheme subunit? Can they substitute for each other or for the cytochrome c_2? What is the primary role of Rpal_4085, the second HiPIP? In this study, we attempted to answer these questions through a combination of genetic, physiological, and biochemical approaches.

MATERIALS AND METHODS

Media and growth conditions for *R. palustris*. *R. palustris* TIE-1 was grown in minimal medium as previously described (15), with the following modifications: the KH_2PO_4 concentration was reduced to 100 μM, and the $NaHCO_3$ concentration was increased to 30 mM. For hydrogen growth, the cooled medium was immediately aliquoted into sealed Balch tubes, and the headspace was flushed with 80% H_2–20% CO_2. Fifty-five to 60% of the vessel was left as headspace, which was pressurized to 5 to 10 lb/in^2. For acetate growth, 10 mM acetate was added to anaerobic medium with a headspace of 80% N_2–20% CO_2. Since the headspace was not required for the electron donor, the bottles were routinely filled almost to the top. For routine aerobic growth, YPS-MOPS growth medium (3 g/liter yeast extract, 3 g/liter peptone, 10 mM dibasic sodium succinate, 50 mM MOPS [morpholinepropanesulfonic acid], adjusted to pH 7 with NaOH) was used.

RNA isolation and qRT-PCR. Culture growth was tracked by measuring the optical density at 650 nm (OD_{650}) of a 0.2-ml sample on a Synergy 4 plate reader (Biotech). Samples with an OD_{650} of 0.3 were used for RNA extraction. Three milliliters of culture was added to 3 ml RNAlater (Ambion) in a Coy anaerobic chamber. Samples were centrifuged for 6 min at 6,000 × *g* and room temperature. The supernatant was poured off, and the pellets were frozen at −80°C until RNA extraction.

Cells were lysed using the lysis, digestion, and mechanical disruption protocol from Qiagen, and RNA purification was performed with a Qiagen RNeasy kit according to the manufacturer's instructions. Purified samples were treated with Ambion Turbo DNase using Ambion's rigorous treatment to remove contaminating DNA and quantified with a NanoDrop spectrophotometer. Forty nanograms of RNA was used to make cDNA using a Bio-Rad cDNA kit. One microliter of the cDNA reaction mixture was assayed in a 25-μl quantitative reverse transcription-PCR (qRT-PCR) reaction mixture using an iTAQ SYBR green Supermix with carboxy-X-rhodamine from Bio-Rad. Standard curves were made using RNA synthesized with an Ambion MEGAscript kit. The resulting RNA was diluted to a known concentration and treated in the same way as the experimental samples. qRT-PCR was performed with a 7500 fast real-time PCR system from Applied Biosystems. Data from four independent cultures were analyzed, and standard curves were generated using Sequence Detection software (version 1.4.0.25).

Construction of deletion and substitution strains. The strains used in this study are listed in Table 1, and the primers used in this study are provided in Table S1 in the supplemental material. To delete *Rpal_4085*, ~1-kb fragments of the upstream and downstream regions were amplified using primer sets HipipUpF2/HipipUpR and HipipDownF/HipipDownR2. These fragments were recombined and cloned into pMQ84 using a *Saccharomyces cerevisiae* cloning system (16). The recombined fragment was cut out of pMQ84 and cloned into the suicide vector pJQ200SK. This vector was transformed into *Escherichia coli* S17-1 and mated into *R. palustris* TIE-1 as previously described (14). The strain in which *pioC* was replaced by *Rpal_4085* was made in a similar fashion: the upstream, signal sequence, and downstream regions of PioC were amplified with the primer sets PioCmchF1C/PiC-HfusionsigR1b and PioC-HfusionsigF2/PioCHfusionR2, and the coding region (without the signal sequence) of *Rpal_4085* was amplified with the primer set PioCHfusionF3/PioCmchR3C.

TABLE 1 Strains used in this work

Rhodopseudomonas palustris strain	Description	Reference or source
TIE-1	Wild-type strain	13
ΔpioC	*R. palustris* TIE-1 Δ*pioC*	14
ΔRpal_4085	*R. palustris* TIE-1 Δ*Rpal_4085*	This study
ΔpioC ΔRpal_4085	*R. palustris* TIE-1 Δ*pioC* Δ*Rpal_4085*	This study
pioC → Rpal_4085	*R. palustris* TIE-1 with replacement of *pioC* by *Rpal_4085*	This study
ΔcycA	*R. palustris* TIE-1 with deletion of cytochrome c_2	This study

The *cycA* deletion strain was made as described above for the *Rpal_4085* mutant using the primer sets Cyc2upF/Cyc2upR and Cyc2ddownF/Cyc2downR. The complementation strain was made in plasmid pBBR-MCS2 using the primers Cyc2CF and Cyc2CR. The PCR product and plasmid were cut with SpeI and HindIII. The ligation was performed with T4 ligase (New England Biolabs), and the resulting plasmid was transformed into *E. coli* DH5α electrocompetent cells. The successfully cloned plasmid was purified and sequenced to confirm that the full sequence was present. The plasmid was transformed into the Δ*cycA* strain and maintained with 100 μg/ml kanamycin.

Cell suspension assay for Fe(II) oxidation. The cell suspension assay for Fe(II) oxidation was performed as previously described (14). Briefly, cells grown on hydrogen were harvested by centrifugation when the OD_{650} was ~0.3, rinsed anaerobically in cell suspension buffer (50 mM HEPES, 20 mM NaCl, 20 mM $NaHCO_3$, pH 7), and resuspended in the same buffer plus ~600 μM $FeCl_2$ to an OD_{650} of ~0.8. One hundred microliters of each sample was aliquoted into a clear flat-bottomed 96-well plate and incubated under a 60-W light bulb. Fifty microliters of samples was taken from a new well at each time point and combined with 50 μl ferrozine solution (0.1% [wt/vol] ferrozine in 50% ammonium sulfate). The absorbance was measured at 570 nm after a 10-min incubation, and the Fe(II) concentration was calculated on the basis of a standard curve.

Cloning, expression, and purification of the HiPIPs. The primers used in this study are listed in Table S1 in the supplemental material. Amplification of *pioC* was achieved by PCR with forward primer PioC-N-NcoCap and reverse primer PioC-C-XhoCap using genomic DNA extracted from aerobically grown *R. palustris* as the template. The PCR product was digested with the restriction enzymes NcoI and XhoI and ligated into the pET32h vector to generate plasmid pET32hPioC. PioC without its signal sequence was PCR amplified from pET32hPioC using forward and reverse primers PioCwithoutTAT and PioC-C-XhoCap, respectively. The resulting PCR product was cloned into pET32h by using NcoI and XhoI restriction enzymes.

The same expression protocol was used for the two proteins. PioC and Rpal_4085 were expressed in *E. coli* BL21 with a pET32h plasmid. The signal sequences predicted with TatP (17) were excluded from the resulting construct: thioredoxin–6× His–thrombin cleavage site–HiPIP. Both strains were grown in LB medium at 37°C. At an OD_{600} of 1, expression was induced with 0.5 mM IPTG (isopropyl-β-D-thiogalactopyranoside)

at 30°C. After 4 h, cells were harvested by centrifugation and resuspended in binding buffer (50 mM phosphate buffer, 300 mM NaCl, pH 8). Cells were lysed with a Thermo Scientific French press at 14,000 lb/in^2, and cell debris was removed by centrifugation. The resulting supernatant was loaded into a Qiagen Ni-nitrilotriacetic acid (NTA) agarose column equilibrated with binding buffer. Bound proteins were eluted with elution buffer (50 mM phosphate buffer, 300 mM NaCl, 250 mM imidazole, pH 8). After elution, the bound fraction was incubated with GE Healthcare thrombin overnight, according to the manufacturer's protocol. The enzymatic digest was dialyzed against binding buffer and reloaded into the reequilibrated Ni-NTA column. Target proteins did not bind to the column and were collected in the flowthrough. Purity was evaluated by SDS-PAGE with Coomassie blue staining. N-terminal sequencing showed that the obtained proteins were correctly digested by thrombin. Concentrations were estimated by UV-visible absorbance spectroscopy assuming a molar extinction coefficient of 16 mM^{-1} cm^{-1} at 396 nm. Nuclear magnetic resonance (NMR) data revealed a homogeneous population of correctly processed protein.

Cyclic voltammetry. Cyclic voltammograms were recorded using an Autolab PSTAT10 potentiostat. The working electrode was a pyrolytic graphite-edge disc, a platinum wire was used as counter electrode, and an Ag/AgCl (1 M KCl) electrode was used as a reference. Reduction potentials are reported versus standard hydrogen electrode (SHE); experimental values were converted to potentials versus SHE by adding +222 mV to the readings made at 25°C. Prior to each experiment, the working electrode was washed with Millipore water (18 MΩ · cm). For each voltammogram, 20 μl of HiPIP at 5 μM in 50 mM Tris HCl, 300 mM NaCl, pH 9, buffer was used. The scan rate was 1 $mV \cdot s^{-1}$. An initial potential of 750 mV was applied to the sample for 10 min before recording of each voltammogram. Data were processed with the SOAS program using a noise filter with an automatic threshold and subtraction of the background current (18).

EPR spectroscopy. The electron paramagnetic resonance (EPR) spectra of pure HiPIPs were recorded on a Bruker EMX spectrometer equipped with a dual-mode cavity and an Oxford Instruments continuous-flow cryostat. The experimental conditions were a temperature of 10 K, a microwave frequency of 9.66 GHz, microwave power of 6.346 mW, a modulation amplitude of 0.5 mT, and a receiver gain of 1.00×10^5. The HiPIP concentration was 200 μM in 100 mM potassium phosphate buffer, 400 mM KCl, pH 8. Sample oxidation was achieved by addition of potassium ferricyanide at concentrations lower than the protein concentration, to avoid artifacts from unreacted ferricyanide.

Membrane fractions were prepared for EPR spectroscopy by two methods: for EPR spectra used in detection of natively expressed HiPIPs, the wild-type strain and the strain in which *pioC* was replaced by *Rpal_4085* strains were grown on minimal medium with H_2-CO_2 to early stationary phase. Cell lysis was performed with the BugBuster reagent (EMD Millipore), according to the manufacturer's protocol, followed by ultracentrifugation at 200,000 × *g*. The pelleted membranes were resuspended in 20 mM phosphate buffer, pH 7, and oxidized with potassium hexachloroiridate(IV).

To prepare membranes for photooxidation experiments with pure proteins, the Δ*pioC* Δ*Rpal_4085* strain was grown anaerobically on minimal acetate medium to early stationary phase. The cell pellets were resuspended in 5 ml of 50 mM potassium phosphate buffer at pH 6 and passed three times through a Thermo Scientific French press at 25,000 lb/in^2. The cell lysate was centrifuged at 10,000 × *g* for 20 min to remove unbroken cells, and the supernatant was ultracentrifuged for 30 min in a Beckman-Coulter TLA-100.3 rotor at 60,000 rpm. The supernatant was discarded, and the pelleted membranes were resuspended in 4 ml of the same buffer. A total of 0.2 ml of 0.5 mM HiPIP solution was mixed with 0.1 ml of membrane suspension in a 3-mm EPR tube. The tubes were incubated for 30 min ~10 cm from a 36-W white fluorescent lamp or in the dark, prior to freezing with liquid N_2.

The spectra of the membrane fractions and of the membrane suspension assay were recorded in a Bruker EMX spectrometer equipped with an ESR-900 continuous-flow helium cryostat. The experimental conditions were a temperature of 13 K, a microwave frequency of 9.39 GHz, microwave power of 2.012 mW, a modulation amplitude of 1 mT, and a receiver gain of 5.02×10^4.

Metal and nonmetal shocks of TIE-1 cultures. To determine the transcriptional response of *Rpal_4085* to metal shocks, we grew 8-ml triplicate cultures anaerobically on minimal medium with acetate to mid-log phase and transferred them to an anoxic chamber. A 5-ml aliquot was removed and added to RNAlater as described above, and the cultures were shocked with either 2 μM $CuCl_2$, 50 μM $NiCl_2$, 1 mM $CoCl_2$, 1 mM $FeCl_2$, 1 mM $MnCl_2$, 1 mM $ZnCl_2$, 300 μM H_2O_2, or 1 mM $CaCl_2$. All metal stocks were prepared in anaerobic water. The concentrations were chosen to reflect the various levels of sensitivity to each compound that *R. palustris* growth displays. Shocked cultures were incubated under light for 20 min, and a second RNA sample was preserved.

Cytochrome c_2 purification. Cytochrome c_2 was purified using a modified version of the native purification protocol described by Bartsch (19). Six liters of *R. palustris* was grown anaerobically on YPS-MOPS medium until stationary phase, harvested, washed in 1/10 volume of 100 mM Tris buffer, pH 8, and resuspended in the same buffer. Cells were lysed using a French press and ultracentrifuged for 1.5 h at 100,000 × *g*. The resulting lysate was fractionated by ammonium sulfate precipitation: ammonium sulfate solution was added to make a 30% solution, and the lysate was stirred for 10 min at 4°C and then centrifuged for 20 min at 25,000 × *g*. Additional ammonium sulfate was added to the supernatant to a final concentration of 90%. The lysate was again stirred and centrifuged, and the resulting pellet was resuspended in 10 mM Tris, pH 8, and desalted using a HiPrep 26/10 desalting column (GE Healthcare) into 1 mM Tris, pH 8.

The enriched cytochrome c_2 sample was further purified using ion-exchange chromatography. The desalted sample was passed through DEAE Sephacel resin (GE Healthcare) using a low-pressure Bio-Rad pump. The flowthrough, which contained cytochrome c_2, was adjusted to pH 5.5 by slow addition of 1 M acetic acid and then passed through CM Sepharose FastFlow resin equilibrated with 1 mM phosphate buffer, pH 6. The column was rinsed with 10 mM phosphate buffer, pH 6, and the protein was eluted with 20 mM Na-phosphate, pH 6. The eluate was diluted to 10 mM phosphate and loaded on a prepacked 1-ml CaptoS FastFlow column using an AKTA purifier fast-performance liquid chromatograph (GE). The column was rinsed with 10 mM Na-phosphate and eluted with 100 mM phosphate buffer, pH 6. The eluate was concentrated to 500 μl using a 3-kDa spin column and run on a gel filtration column as a final polishing step. The final protein was checked for purity by UV-visible spectra and run on an SDS-polyacrylamide gel stained with Coomassie.

Cytochrome c_2 titration. Cytochrome c_2 from *R. palustris* TIE-1 was titrated in a Cary 5 UV/visible spectrophotometer using a home-built optical titration cell as described by Dutton (20). Cytochrome c_2 (100 μM) was titrated in the presence of the following redox mediators (in 50 mM MOPS at pH 7): ferrocene, *p*-benzoquinone, 2,5-dimethyl-*p*-benzoquinone, and 1,2-naphthoquinone (all at 20 μM) as well as 2,6-dichlorophenolindophenol at 5 μM. Ferricyanide and dithionite were added to, respectively, increase and lower the ambient midpoint potential.

Electron transfer from purified proteins in membrane fragments. Membrane fragments for reaction center reduction studies were prepared from acetate-grown cultures. Late-log-phase cells were lysed by 2 French press passages, spun at low speed to remove unbroken cells, and ultracentrifuged for 1 h at 150,000 × *g*. Membranes were rinsed once in 50 mM MOPS, pH 7, and resuspended in the same buffer.

Membrane suspensions were added to a round, stoppered quartz cuvette and measured on a Joliot type Jts-10 flash-induced spectrometer (Bio-Logic). Membrane-protein interactions were measured in the presence of ascorbate and myxothiazol to provide a reducing environment and inhibit the cytochrome bc_1 complex, respectively. Ascorbate was

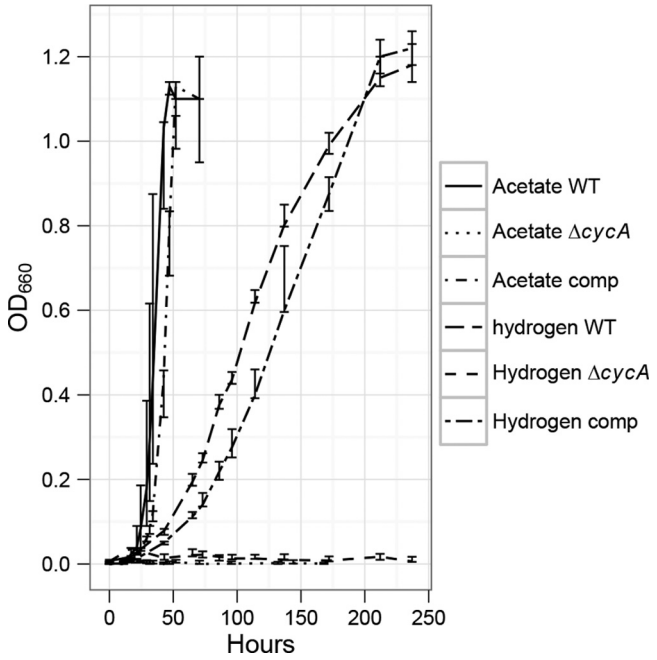

FIG 1 Wild-type (WT) TIE-1, the Δ*cycA* mutant, and the Δ*cycA* mutant complemented with *cycA-pbbR* (comp) growing photoheterotrophically on minimal medium with acetate and photoautotrophically with H_2-CO_2. While wild-type TIE-1 was able to grow under both conditions, the Δ*cycA* mutant was not, while the complemented strain showed restored growth. The lines indicate the median values of 3 independent biological cultures, and the error bars represent the data range.

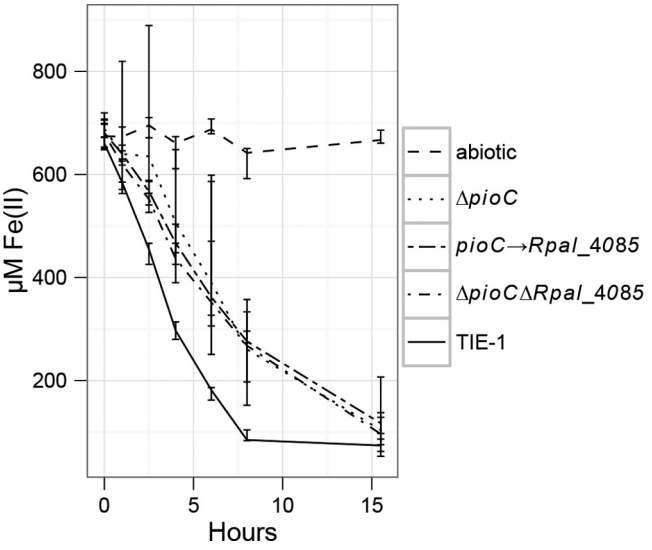

FIG 2 Fe(II) oxidation rates of TIE-1 and mutant strains grown on minimal medium with hydrogen as the electron donor. Lines are the medians of 4 independent biological cultures, while the error bars show the range. The single Δ*Rpal_4085* mutant (not shown) oxidized Fe(II) at the same rate as wild-type TIE-1.

added from a 0.5 M stock solution. Myxothiazol was added from a 10 mM stock dissolved in ethanol and stored at −20°C. The reaction centers in the membrane fragments were photooxidized using a saturating flash from a custom-made (Daniel Beal, JBeamBio, France) light ring of actinic light-emitting diodes (800 nm), and changes in the absorbance at 435 nm (mainly originating from the photooxidized pigment) and 420 nm (dominated by redox changes of cytochrome c_2) were recorded. We chose to monitor cytochrome oxidation through changes at 420 nm because the change in alpha band absorption was obscured by electrochromic absorption changes in the same region. Spectral deconvolution was performed on the basis of the analysis of time-resolved flash-induced spectra, which will be described in a separate article (L. J. Bird, J. Lavergne, W. Nitschke, and D. K. Newman, unpublished data) focusing on whole-cell and *in vitro* analysis of light-induced electron transfer in *R. palustris* TIE-1.

RESULTS

Mutant analysis. Cytochrome c_2 is a common periplasmic electron shuttle between the cytochrome bc_1 complex and the reaction center; however, in some organisms, HiPIPs also assume this role (6). Given that TIE-1 has two HiPIPs as well as cytochrome c_2, we wanted to determine whether cytochrome c_2 is required for phototrophic growth. Accordingly, we made a clean deletion of the gene encoding cytochrome c_2 (*cycA*) and tested the resulting mutant strain for phototrophic growth with acetate or hydrogen as the electron donor. The Δ*cycA* mutant could not grow under these conditions, demonstrating that cytochrome c_2 is essential for photosynthesis in TIE-1 and that it cannot be replaced by either HiPIP (Fig. 1). The Δ*cycA* mutant also did not grow in the presence of Fe(II)-NTA; however, because TIE-1 growth on Fe(II) is unreliable when inoculated from an anaerobic culture, this result is not entirely conclusive.

We next sought to determine whether the HiPIPs PioC and Rpal_4085 could substitute for each other. Previous work had shown that although the TIE-1 Δ*pioC* mutant is unable to grow using Fe(II) as an electron donor, it still has some Fe(II) oxidation activity (14). We hypothesized that the residual Fe(II) oxidation activity might be due to the presence of another HiPIP (Rpal_4085) in the Δ*pioC* mutant, given that diverse proteins are known to donate electrons to the reaction center in other bacteria (21). To test this hypothesis, we deleted *Rpal_4085* in both the wild-type and Δ*pioC* mutant backgrounds. The results were unexpected: the Δ*pioC* Δ*Rpal_4085* mutant was able to oxidize Fe(II) at the same rate as the Δ*pioC* mutant (Fig. 2), while the Δ*Rpal_4085* mutant grew on and oxidized Fe(II) at the same rate as the wild type. This suggests that Rpal_4085 does not substitute for PioC in the Fe(II) oxidation pathway. Given that both proteins are small redox-active proteins in the same family, we wondered why Rpal_4085 does not at least partially substitute for PioC in the iron oxidation pathway.

To determine whether Rpal_4085's inability to substitute for PioC was due to a lack of protein expression and/or a difference in localization between the two HiPIPs, we replaced the coding region of *pioC* with the coding region of *Rpal_4085*, leaving the twin arginine translocation (TAT) signal sequence of *pioC* intact. We used qRT-PCR to determine whether the mutant in which *pioC* was replaced by *Rpal_4085* was properly expressing the *Rpal_4085* gene. We found that in the wild-type strain grown on H_2, *Rpal_4085* expression was significantly lower than *pioC* expression. In the mutant in which *pioC* was replaced by *Rpal_4085*, the expression of *Rpal_4085* was increased to within the range of *pioC* expression in TIE-1 (Table 2). EPR spectroscopy of strains with a wild-type *pioC* operon and the substitution of *Rpal_4085* for *pioC* indicated that HiPIP was present at very low levels in both samples (see Fig. S1 in the supplemental material). The resulting mutant (in which *pioC* was replaced by *Rpal_4085*) oxidized Fe(II) at the same rate as the Δ*pioC* mutant as shown in Fig. 2. This result

TABLE 2 Transcript quantitation for cultures used in Fig. 2

Strain	Gene	No. of copies/ng		
		Median	Minimum	Maximum
Wild type	*Rpal_4085*	4,790	960	10,790
Mutant with *pioC* replaced by *Rpal_4085*	*Rpal_4085*	328,440	203,120	494,380
Wild type	*pioC*	10,028,440	57,060	1,080,000

strongly suggested that the Rpal_4085 protein cannot take on PioC's role in Fe(II) oxidation. This raised the following question: what is the biochemical basis of Rpal_4085's inability to substitute for PioC? As a step toward answering this question, we purified and characterized cytochrome c_2 and both HiPIPs.

HiPIP purification and EPR spectroscopy. We used EPR spectroscopy for two purposes: (i) to verify that both PioC and Rpal_4085 are typical HiPIPs and (ii) to determine whether they could be oxidized by the photosynthetic reaction center. We first expressed and purified the two HiPIPs from TIE-1 using a fusion with His-tagged thioredoxin. Because thioredoxin is placed at the N terminus, the periplasmic TAT signal sequence of the HiPIPs was removed in the cloning so the fusion protein would accumulate in the cytoplasm. This strategy, followed by affinity chromatography and proteolytic cleavage of thioredoxin, resulted in pure HiPIPs with a yield of 3 mg/liter culture. NMR experiments showed no evidence of significant amounts of apoprotein or of protein with an incorrectly assembled Fe-S cluster. EPR spectroscopy on pure protein confirmed that both PioC and Rpal_4085 displayed the characteristics of typical HiPIPs. This technique detects the presence of unpaired electrons which, in the case of metal clusters, have different spectral characteristics, depending on the nature of the cluster. Reduced HiPIPs have a diamagnetic ground state. Because only the ground state is occupied at the temperature of the EPR spectroscopy experiments, both proteins were EPR spectroscopy silent in the reduced form (not shown). In the oxidized form, the ground state is paramagnetic and HiPIPs display a characteristic EPR spectrum (22) (Fig. 3). The spectra in Fig. 3 show the characteristic signals of HiPIPs, where the main features have g values (proportionality constants, which reflect the environment of the electrons detected) of 2.12 and 2.03 for PioC and 2.12 and 2.04 for Rpal_4085. Both HiPIPs showed minor species, with the maximum g value being 2.08. These features are typical of HiPIPs and indicate that our purified proteins were correctly processed and active.

To test the ability of each HiPIP to donate electrons to the reaction center, we incubated a reduced sample of each protein with a suspension of membranes from the Δ*pioC* Δ*Rpal_4085* mutant either under light or in the dark. Because only oxidized HiPIPs show the characteristic EPR spectra, the detection of HiPIP by EPR spectroscopy in these experiments indicated that the protein could be oxidized by the reaction center. As observed through EPR spectroscopy (Fig. 4), PioC, but not Rpal_4085, is oxidized by the membrane suspension in a light-dependent manner.

Reduction potentials of HiPIPs and cytochrome c_2. We further characterized PioC and Rpal_4085 by measuring their reduction potentials. The reduction potentials were determined at pH 9 by cyclic voltammetry using a scan rate of 1 mV s^{-1} (Fig. 5). Both proteins showed reversible reactions with midpoint potentials of +450 mV (PioC) and +470 mV (Rpal_4085). Faster scan rates resulted in irreversible reactions. At pH 7, scans were also irreversible, possibly due to poor interaction between the HiPIPs and the electrodes used.

The reduction potential of cytochrome c_2 was determined through optical redox titration, and cytochrome c_2 was found to have a midpoint potential of +350 mV.

Reduction of photooxidized reaction center with pure proteins. Once we had confirmed the identities and determined the reduction potentials of the proteins, we further explored the interaction of the reaction center with cytochrome c_2 and PioC by using flash-induced absorbance spectrometry. We were able to monitor the absorbance changes caused by photooxidation and rereduction of membrane fragments in the presence of PioC or cytochrome c_2. In order to reduce all components prior to each experiment, ascorbate was added to the reaction mixture. Myxothiazol was used to inhibit the cytochrome bc_1 complex present in membrane fragments to ensure that cyclic electron flow did not take place, as this would have complicated the analysis. Because the EPR spectroscopy experiments with membranes indicated that Rpal_4085 could not reduce the reaction center at all, this experiment was not pursued for this protein.

A full description of the light-induced optical changes observed in TIE-1 will be published elsewhere (Bird et al., unpublished). For the present analysis, however, we used the relevant spectral parameters (peak wavelengths and extinction coefficients) obtained during this general spectroscopic and kinetic study to analyze the reactivities of cytochrome c_2 and PioC with the photosynthetic reaction centers (Fig. 6). Figures 6A and B

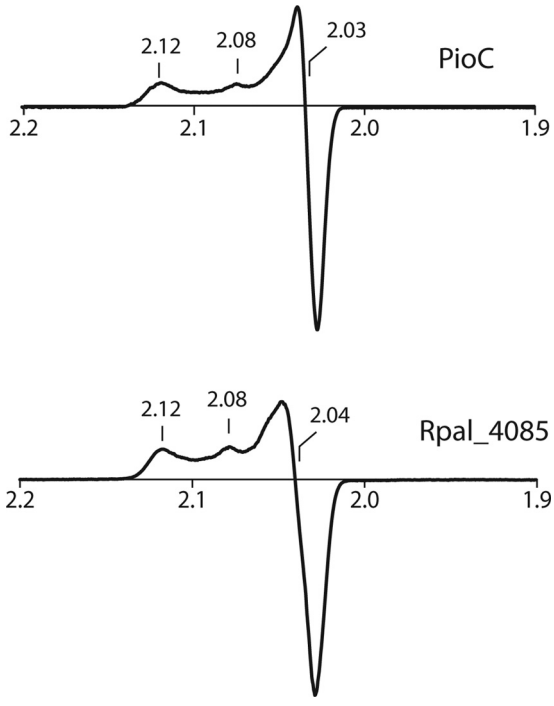

FIG 3 X-band (9.66-GHz) EPR spectra of oxidized purified PioC and Rpal_4085. The g values (which reflect the environment of the electron detected) of the main features of the two HiPIPs are indicated. The features shown here are typical of those of correctly processed HiPIP proteins. The *y* axis is arbitrary and hence is not shown.

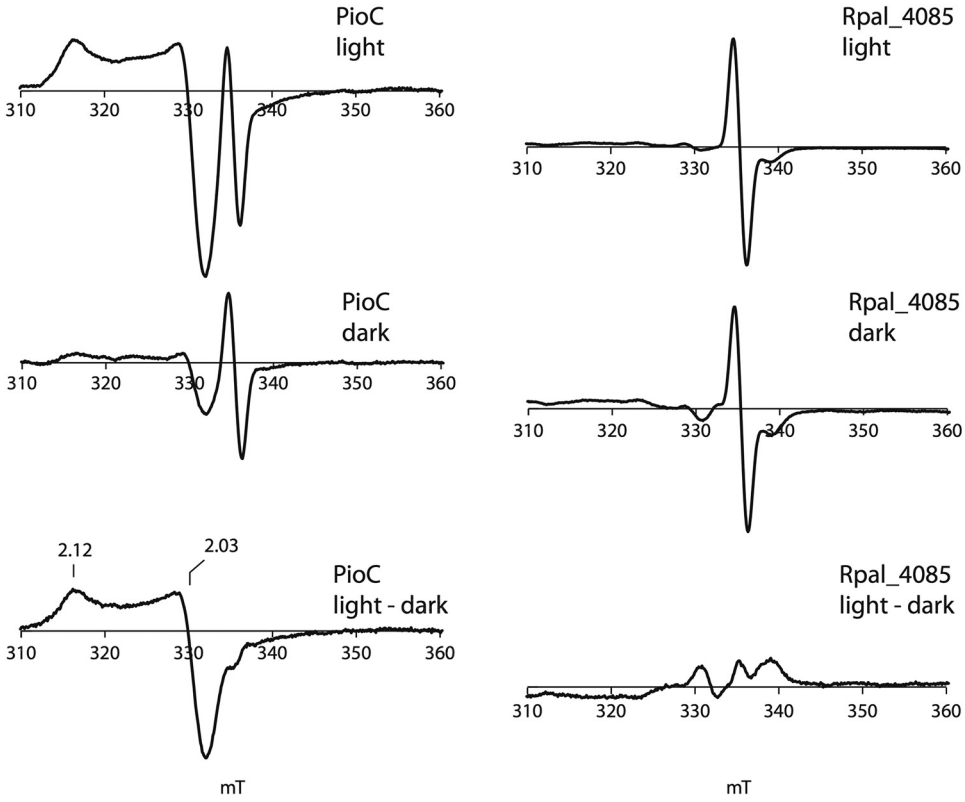

FIG 4 X-band (9.39-GHz) EPR spectra of PioC incubated with a suspension of membranes of the Δ*pioC* Δ*Rpal_4085* mutant in the dark and under light. The HiPIP features are visible for PioC in the membranes incubated in the light and in the difference spectra. Because the peaks that denote a HIPIP are visible only when the protein is oxidized, these results show that membranes are able to oxidize PioC in the presence of light (left). This result was not observed for Rpal_4085 (shown on the right), indicating that it does not interact with the reaction center. The *y* axis is arbitrary and hence is not shown.

compare the rereduction kinetics of the photooxidized primary donor (P^+) in the reaction center in samples equilibrated with low, intermediate, and saturating concentrations of cytochrome c_2 and PioC, respectively, prior to the flash that triggered the reaction. These kinetics demonstrate that cytochrome c_2 and PioC differ significantly in their binding to and reaction with the reaction center.

Both PioC and cytochrome c_2 were able to reduce the photooxidized reaction center (Fig. 6A and B). Kinetic titrations with cytochrome c_2 showed an increase in the rate constant to a maximum of 200 s^{-1} as the cytochrome concentration increased, indicating that the interaction between cytochrome c_2 and the reaction center is collisional (a pseudo-first-order reaction). The fact that only 50% of P^+ was rereduced by cytochrome c_2 even at saturating concentrations of c_2 (Fig. 6A and B, inset) suggests that the membranes are present as equimolar populations of inside-out and right-side-out vesicles produced during the French press treatment. In contrast to cytochrome c_2, PioC's reduction of the reaction center had a time constant ($k = 15\ s^{-1}$) that was independent of the concentration (Fig. 6B), indicating that it forms a complex with the reaction centers prior to the flash. The extent of PioC's donation to the reaction center, on the other hand, was concentration dependent (Fig. 6B, inset). Even at saturating concentrations of PioC, only roughly 60% of the accessible P^+ (the population present in inside-out vesicles) was rereduced in a PioC-dependent manner. The supersaturating population of PioC therefore reduces only part of the photooxidized reaction center, demonstrating that PioC must be close to equipotential with the reduced/oxidized primary donor couple and that the observed kinetics correspond to achievement of redox equilibration rather than the intrinsic electron transfer rate, a parameter that can be observed only if a sufficient driving force (that is, a difference in redox midpoint potentials) for forward electron transfer is present. The strong binding of PioC to the reaction center was consistent with the characteristics of other HiPIPs (23), and redox equilibration between PioC and the reaction center was again consistent with the unusually high redox potential of PioC and the typically observed range of redox potentials for the primary donor pigment of the purple bacterial reaction (24).

Rpal_4085 transcriptional response to divalent cations. Unlike PioC and cytochrome c_2, Rpal_4085 cannot be oxidized by the reaction center. We therefore looked for insight into its function by investigating its transcriptional response to metal stress. In a previously performed microarray (25), Rpal_4085 was upregulated by an anoxic Fe (II) shock, while PioC was not. We therefore hypothesized that it might be involved in mitigating metal toxicity. Using qRT-PCR, we tested the response of Rpal_4085 under anoxic conditions to the cations Mn(II), Fe(II), Co(II), Ni(II), Cu(II), Zn(II), Ca(II), and hydrogen peroxide (H_2O_2). With the exception of Zn(II) and Ca(II), these divalent metals are known to be redox active at physiological pH (19, 26–29). We used H_2O_2 as an oxidative stress-inducing control and Zn(II) and Ca(II) as nonredox active divalent metal controls. We found that in TIE-1 cultures grown on acetate, Rpal_4085 was highly upregulated in response to a shock with Mn(II), Fe(II), Co(II), and Ni(II) but not

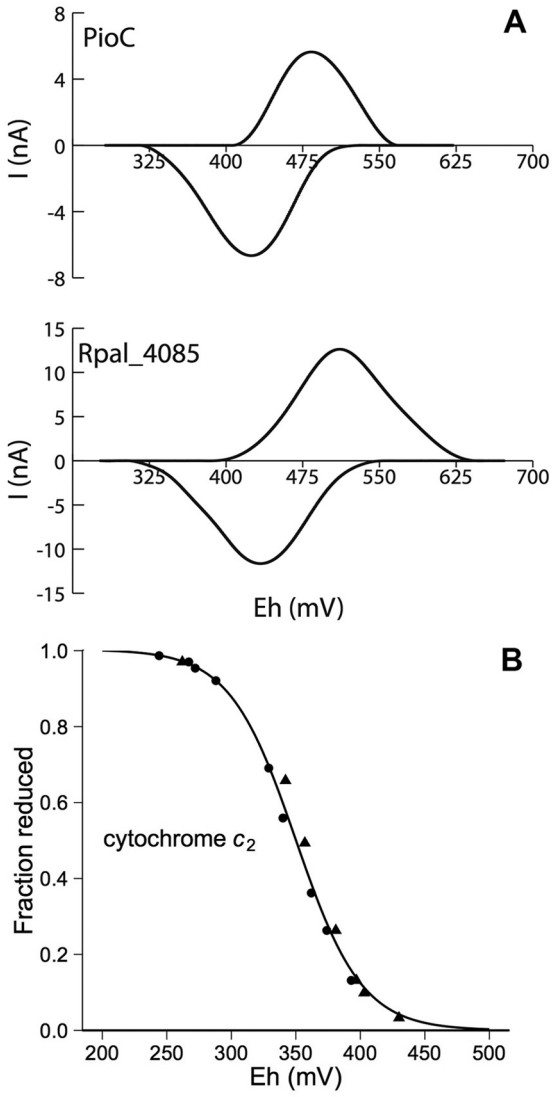

FIG 5 (A) Cyclic voltammograms of PioC and Rpal_4085. The experiments were performed at 25°C with a 1-mV s^{-1} scan rate in 100 mM potassium phosphate buffer, 300 mM NaCl, pH 9. The potentials are reported versus those for the standard hydrogen electrode. The midpoint potential for PioC was 450 mV, and that for Rpal_4085 was 480 mV. The protein concentration was 10 μM. The *y* axis shows current. (B) Optical redox titration of the alpha band of cytochrome c_2 at pH 7.0. Triangles and circles represent data points taken while titrating in the oxidizing and reducing directions, respectively. The line represents a Nernst fit at *n* equal to 1 to the measured data points, yielding a midpoint redox potential of +350 mV.

in response to a shock with Zn(II) or Ca(II) (see Fig. S2 in the supplemental material).

DISCUSSION

R. palustris TIE-1 expresses two HiPIPs (PioC and Rpal_4085) and a cytochrome c_2 during anaerobic growth. In other phototrophic organisms, members of both protein families perform the same function, acting as an electron shuttle in cyclic electron flow (4). We here show that in TIE-1, cytochrome c_2 and PioC have nonoverlapping functions and only cytochrome c_2 acts in cyclic electron flow to support photosynthetic growth, while Rpal_4085 cannot substitute for either of the other proteins.

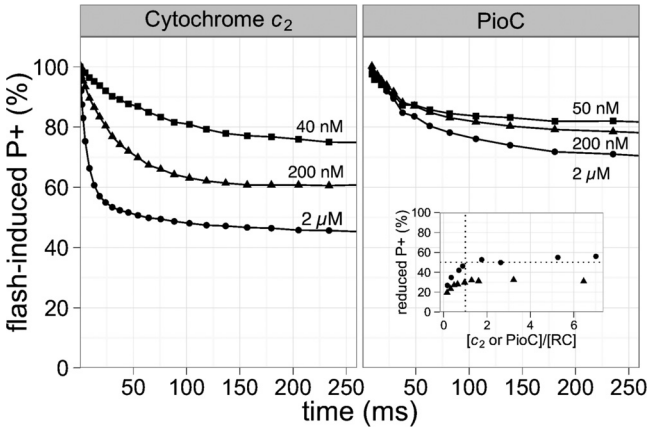

FIG 6 Rereduction of the flash-oxidized reaction center primary donor (P^+) in membrane fragments by purified cytochrome c_2 (A) and PioC (B). The depicted kinetics represent the changes in the absorbance measured at 435 nm with kinetic rereduction phases due to ascorbate and back reaction from the semireduced acceptor quinone B subtracted out to emphasize the reactions of the photosystem with its soluble electron donor proteins. A detailed spectral and kinetic analysis of the donation reaction both in whole cells and in reconstituted systems will be presented in a dedicated publication (Bird et al., unpublished). Kinetic traces corresponding to low, intermediate, and saturating concentrations of the soluble donors are denoted by squares, triangles, and circles, respectively. The primary donor concentration was 260 nM for panel A and 320 nM for panel B. (Inset) Dependence of maximal rereduction of the primary donor pigment on the ratio of cytochrome c_2 (circles) and PioC (triangles) to the reaction center (RC).

Cytochrome c_2 has been extensively studied in several purple bacterial species (28, 30, 31), and the protein found in TIE-1 appears to be typical of this family. Its reduction potential (+350 mV) is typical of cytochromes c_2, and our experiments with purified protein and membrane fragments show that the electron transfer rate from cytochrome c_2 to the reaction center is within the range found in other purple bacteria (8, 32). A *cycA* mutant was unable to grow phototrophically, indicating that cytochrome c_2 is the dominant donor to the reaction center during photosynthetic growth and that neither HiPIP can take on this role. Although this result was not surprising, it required testing because the purple bacterium *Rubrivivax gelatinosus* was recently found to have a HiPIP and three cytochrome *c*-type proteins that function in cyclic electron flow to various degrees (9).

Because the TIE-1 HiPIPs cannot function in cyclic electron flow, they must have other functions. Previous genetic studies showed that PioC has a clear role in Fe(II) oxidation (14, 33) and is essential for photoferrotrophic growth. The resulting model for iron oxidation predicted that PioC would donate either directly or indirectly to the reaction center (Fig. 7). Our results suggest that PioC likely donates directly to the reaction center and not indirectly via cytochrome c_2. This conclusion is supported by the fact that PioC's redox potential is 100 mV higher than that of cytochrome c_2 and by PioC's ability to be oxidized by membranes lacking any measurable cytochrome c_2. Furthermore, the fact that the rate of electron transfer between PioC and the reaction center remains constant with increasing concentrations of PioC suggests that PioC binds to the reaction center.

Reduction potentials for reaction centers in purple bacteria range from +430 to +500 mV (24, 34); PioC's reduction potential (+450 mV) is within this range, making it nearly isopotential with

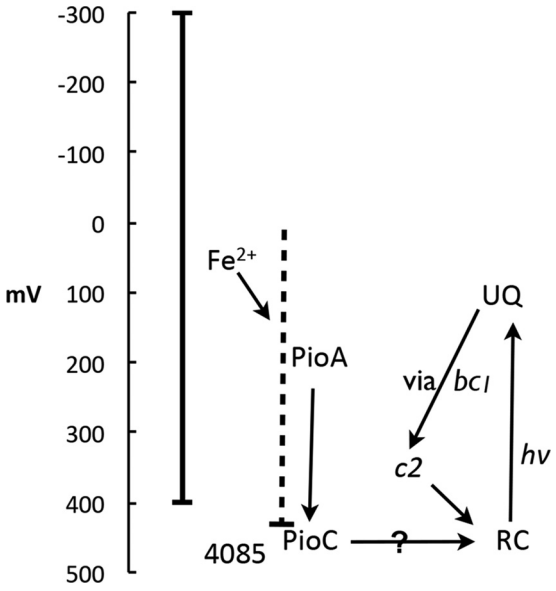

FIG 7 Electron flowchart in *R. palustris* TIE-1. The *y* axis denotes the reduction potential of the various components. Solid arrows, predicted electron flow; vertical solid line, potential range of known forms of Fe(II); dashed line, possible reduction potential range of PioA, which has not been determined; the possible range is constrained by the range required for iron oxidation and by the known potential range of related decaheme proteins. hv, energy provided by a photon; UQ, ubiquinone.

the reaction center. It therefore seems probable that the rate of electron transfer observed from PioC (15 s^{-1}) is the rate of equilibration rather than the true rate of electron transfer. At first sight, PioC being about equipotential with the reaction center primary donor may appear to be counterintuitive because it would preclude efficient forward electron transfer. This situation, however, is specific to the (nonphysiological) conditions of our single-turnover flash experiments. In TIE-1 cells exposed to continuous light, a small number of consecutive photooxidation events result in quantitative oxidation of the bound population of PioC. The unusually high redox potential of PioC may result from a compromise imposed by its being at the same time an electron acceptor of the Fe-oxidizing system (requiring PioC to be a strong oxidant) and an electron donor to the reaction centers's primary donor pigment.

Our results indicate that PioC binds to and reduces the reaction center, consistent with the model shown in Fig. 7. The rate of PioC reduction appears to be substantially lower than that of cytochrome c_2. Our EPR spectroscopy results with membrane fragments (see Fig. S1 in the supplemental material) indicate that PioC is not highly expressed in whole cells. These facts combined suggest that the reaction center is reduced, on average, predominantly by cytochrome c_2 and not by PioC. These differences in the rates and strengths of binding may be part of a cellular strategy to balance energy production (cyclic electron flow) with electron acquisition from iron.

Although they are different with respect to sequence (35% identical and 65% similar over 54 amino acids, excluding the TAT sequences), PioC and Rpal_4085 are similar spectroscopically, show the typical EPR patterns of HiPIPs, and have similar reduction potentials. However, the lack of interaction between Rpal_4085 and the reaction center indicates that this protein does not function in photosynthesis. Rpal_4085's inability to be oxidized by illuminated membrane fragments may be a function of its reduction potential: although it is only 20 mV higher than that of PioC, this difference might make Rpal_4085 unable to efficiently donate to the reaction center. It is, of course, possible that other factors, such as a lack of binding between Rpal_4085 and the reaction center, are responsible for our observations.

So, what role might Rpal_4085 play? There are examples of HiPIPs in nonphototrophic organisms that interact with the cytochrome bc_1 complex during respiration, such as those in *Rhodothermus marinus* (35, 36) and *Acidithiobacillus ferrooxidans* (37, 38). It is possible that Rpal_4085 serves a similar function in *R. palustris* respiration, although the Δ*Rpal_4085* mutant had no defect when growing aerobically on acetate and succinate under standard growth conditions. Another possible role for Rpal_4085 is suggested by the fact that its expression is upregulated by Mn(II), Fe(II), Co(II), and Ni(II) (see Fig. S1 in the supplemental material). This response may indicate that Rpal_4085 acts as a periplasmic sensor for divalent, oxidizable metals or may even play a role in metal detoxification. Other (non-HiPIP) iron sulfur proteins act as redox sensors (39), making such a role for Rpal_4085 seem feasible. More research will be needed to determine the function of Rpal_4085 in *R. palustris*.

In summary, this work demonstrates that three soluble electron donors in *R. palustris* TIE-1 play distinct roles in TIE-1. The function of cytochrome c_2 is in cyclic electron transfer for photosynthetic energy generation by shuttling electrons from the cytochrome bc_1 complex to the reaction center. The two HiPIPs are biochemically similar, but only one, PioC, is capable of donating electrons to the reaction center. The second HiPIP, Rpal_4085, appears to have an entirely different function, possibly related to metal homeostasis. More studies are required to fully elucidate the *in vivo* roles of PioC and Rpal_4085 and to understand the physical differences between the two proteins.

ACKNOWLEDGMENTS

The N-terminal data were provided by the Analytical Laboratory, Analytical Services Unit, Instituto de Tecnologia Química e Biológica, Universidade Nova de Lisboa. We thank Pablo Gonzales at FCT-UNL for the EPR spectra of pure HiPIPs and Miguel Teixeira at ITQB for obtaining the other EPR data and for helpful discussions. We thank J. Lavergne (Cadarache, France) for advice on kinetic experiments.

We thank the Howard Hughes Medical Institute (HHMI) and the MIT-Portugal Program (MIT-Pt/BS-BB/0014/2008) for supporting this work. D.K.N. is an HHMI investigator, and L.J.B. was a PEO scholar. This work was also supported by FCT through grant PEst-OE/EQB/LA0004/2011 and grant PTDC/BIA-PRO/098158/2008. I.H.S. is the recipient of FCT grant SFRH/BD/36582/2007.

REFERENCES

1. **Meyer TE, Cusanovich MA.** 2003. Discovery and characterization of electron transfer proteins in the photosynthetic bacteria. Photosynth. Res. **76:**111–126. http://dx.doi.org/10.1023/A:1024910323089.
2. **Heering HA, Bulsink BM, Hagen WR, Meyer TE.** 1995. Influence of charge and polarity on the redox potentials of high-potential iron-sulfur proteins: evidence for the existence of two groups. Biochemistry **34:** 14675–14686. http://dx.doi.org/10.1021/bi00045a008.
3. **Reedy CJ, Elvekrog MM, Gibney BR.** 2008. Development of a heme protein structure-electrochemical function database. Nucleic Acids Res. **36**(Database Issue):D307–D313. http://dx.doi.org/10.1093/nar/gkm814.
4. **Van Driessche G, Vandenberghe I, Devreese B, Samyn B, Meyer TE, Leigh R, Cusanovich MA, Bartsch RG, Fischer U, Van Beeumen JJ.** 2003. Amino acid sequences and distribution of high-potential iron-

sulfur proteins that donate electrons to the photosynthetic reaction center in phototropic proteobacteria. J. Mol. Evol. **57:**181–199. http://dx.doi.org/10.1007/s00239-003-2465-y.
5. **Lieutaud C, Alric J, Bauzan M, Nitschke W, Schoepp-Cothenet B.** 2005. Study of the high-potential iron sulfur protein in Halorhodospira halophila confirms that it is distinct from cytochrome c as electron carrier. Proc. Natl. Acad. Sci. U. S. A. **102:**3260–3265. http://dx.doi.org/10.1073/pnas.0407768102.
6. **Menin L, Gaillard J, Parot P, Schoepp B, Nitschke W, Vermeglio A.** 1998. Role of HiPIP as electron donor to the RC-bound cytochrome in photosynthetic purple bacteria. Photosynth. Res. **55:**343–348. http://dx.doi.org/10.1023/A:1005989900756.
7. **Menin L, Schoepp B, Parot P, Vermeglio A.** 1997. Photoinduced cyclic electron transfer in *Rhodocyclus tenuis* cells: participation of HiPIP or cyt c8 depending on the ambient redox potential. Biochemistry **36:**12183–12188. http://dx.doi.org/10.1021/bi971163b.
8. **Gong XM, Paddock ML, Okamura MY.** 2003. Interactions between cytochrome c(2) and photosynthetic reaction center from Rhodobacter sphaeroides: changes in binding affinity and electron transfer rate due to mutation of interfacial hydrophobic residues are strongly correlated. Biochemistry **42:**14492–14500. http://dx.doi.org/10.1021/bi035603c.
9. **Ohmine M, Matsuura K, Shimada K, Alric J, Vermeglio A, Nagashima KVP.** 2009. Cytochrome c(4) can be involved in the photosynthetic electron transfer system in the purple bacterium Rubrivivax gelatinosus. Biochemistry **48:**9132–9139. http://dx.doi.org/10.1021/bi901202m.
10. **Hochkoeppler A, Zannoni D, Ciurli S, Meyer TE, Cusanovich MA, Tollin G.** 1996. Kinetics of photo-induced electron transfer from high-potential iron-sulfur protein to the photosynthetic reaction center of the purple phototroph Rhodoferax fermentans. Proc. Natl. Acad. Sci. U. S. A. **93:**6998–7002. http://dx.doi.org/10.1073/pnas.93.14.6998.
11. **Schoepp B, Parot P, Menin L, Gaillard J, Richaud P, Vermeglio A.** 1995. In vivo participation of a high potential iron-sulfur protein as electron donor to the photochemical reaction center of Rubrivivax gelatinosus. Biochemistry **34:**11736–11742. http://dx.doi.org/10.1021/bi00037a010.
12. **Vermeglio A, Nagashima S, Alric J, Arnoux P, Nagashima KV.** 2012. Photo-induced electron transfer in intact cells of Rubrivivax gelatinosus mutants deleted in the RC-bound tetraheme cytochrome: insight into evolution of photosynthetic electron transport. Biochim. Biophys. Acta **1817:**689–696. http://dx.doi.org/10.1016/j.bbabio.2012.01.011.
13. **Jiao Y, Kappler A, Croal LR, Newman DK.** 2005. Isolation and characterization of a genetically tractable photoautotrophic Fe(II)-oxidizing bacterium, Rhodopseudomonas palustris strain TIE-1. Appl. Environ. Microbiol. **71:**4487–4496. http://dx.doi.org/10.1128/AEM.71.8.4487-4496.2005.
14. **Jiao Y, Newman DK.** 2007. The pio operon is essential for phototrophic Fe(II) oxidation in Rhodopseudomonas palustris TIE-1. J. Bacteriol. **189:**1765–1773. http://dx.doi.org/10.1128/JB.00776-06.
15. **Croal LR, Johnson CM, Beard BL, Newman DK.** 2004. Iron isotope fractionation by Fe(II)-oxidizing photoautotrophic bacteria. Geochim. Cosmochim. Acta **68:**1227–1242. http://dx.doi.org/10.1016/j.gca.2003.09.011.
16. **Shanks RMQ, Caiazza NC, Hinsa SM, Toutain CM, O'Toole GA.** 2006. Saccharomyces cerevisiae-based molecular tool kit for manipulation of genes from gram-negative bacteria. Appl. Environ. Microbiol. **72:**5027–5036. http://dx.doi.org/10.1128/AEM.00682-06.
17. **Bendtsen JD, Nielsen H, Widdick D, Palmer T, Brunak S.** 2005. Prediction of twin-arginine signal peptides. BMC Bioinformatics **6:**167. http://dx.doi.org/10.1186/1471-2105-6-167.
18. **Fourmond V, Hoke K, Heering HA, Baffert C, Leroux F, Bertrand P, Leger C.** 2009. SOAS: a free program to analyze electrochemical data and other one-dimensional signals. Bioelectrochemistry **76:**141–147. http://dx.doi.org/10.1016/j.bioelechem.2009.02.010.
19. **Bartsch RG.** 1971. Cytochromes: bacterial. Methods Enzymol. **23:**344–363.
20. **Dutton PL.** 1971. Oxidation-reduction potential dependence of the interaction of cytochromes, bacteriochlorophyll and carotenoids at 11°K in chromatophores of Chromatium D and Rhodopseudomonas gelatinosa. Biochim. Biophys. Acta **226:**63–80. http://dx.doi.org/10.1016/0005-2728(71)90178-2.
21. **Nagashima S, Shimada K, Vermeglio A, Nagashima KV.** 2011. The cytochrome c(8) involved in the nitrite reduction pathway acts also as electron donor to the photosynthetic reaction center in Rubrivivax gelatinosus. Biochim. Biophys. Acta **1807:**189–196. http://dx.doi.org/10.1016/j.bbabio.2010.10.020.
22. **Priem AH, Klaassen AA, Reijerse EJ, Meyer TE, Luchinat C, Capozzi F, Dunham WR, Hagen WR.** 2005. EPR analysis of multiple forms of [4Fe-4S](3+) clusters in HiPIPs. J. Biol. Inorg. Chem. **10:**417–424. http://dx.doi.org/10.1007/s00775-005-0656-2.
23. **Lieutaud C, Nitschke W, Vermeglio A, Parot P, Schoepp-Cothenet B.** 2003. HiPIP in Rubrivivax gelatinosus is firmly associated to the membrane in a conformation efficient for electron transfer towards the photosynthetic reaction centre. Biochim. Biophys. Acta **1557:**83–90. http://dx.doi.org/10.1016/S0005-2728(02)00397-3.
24. **Nitschke W, Dracheva SM.** 1995. Reaction center associated cytochromes, p 775–805. *In* Blankenship RE, Madigan MT, Bauer CE (ed), Anoxygenic photosynthetic bacteria. Kluwer Academic Publishers, Dordrecht, Netherlands.
25. **Bird LJ, Coleman ML, Newman DK.** 2013. Iron and copper act synergistically to delay anaerobic growth in bacteria. Appl. Environ. Microbiol. **79:**3619–3627. http://dx.doi.org/10.1128/AEM.03944-12.
26. **Barras F, Fontecave M.** 2011. Cobalt stress in Escherichia coli and Salmonella enterica: molecular bases for toxicity and resistance. Metallomics **3:**1130–1134. http://dx.doi.org/10.1039/c1mt00099c.
27. **Macomber L, Hausinger RP.** 2011. Mechanisms of nickel toxicity in microorganisms. Metallomics **3:**1153–1162. http://dx.doi.org/10.1039/c1mt00063b.
28. **Lavergne J, Vermeglio A, Joliot P.** 2009. Functional coupling between reaction centers and cytochrome *bc*1 complexes. *In* Hunter N, Daldal F, Thurnauer M, Beatty T (ed), The purple phototrophic bacteria. Springer, Dordrecht, Netherlands.
29. **Touati D.** 2000. Iron and oxidative stress in bacteria. Arch. Biochem. Biophys. **373:**1–6. http://dx.doi.org/10.1006/abbi.1999.1518.
30. **Axelrod H, Miyashita O, Okamura M.** 2009. Structure and function of cytochrome *c2*: reaction center complex from *Rhodobacter sphaeroides*, p 323–336. *In* Hunter N, Daldal F, Thurnauer M, Beatty T (ed), The purple phototrophic bacteria. Springer, Dordrecht, Netherlands.
31. **Wang S, Li X, Williams JC, Allen JP, Mathis P.** 1994. Interaction between cytochrome c2 and reaction centers from purple bacteria. Biochemistry **33:**8306–8312. http://dx.doi.org/10.1021/bi00193a018.
32. **Knaff DB, Willie A, Long JE, Kriauciunas A, Durham B, Millett F.** 1991. Reaction of cytochrome c2 with photosynthetic reaction centers from Rhodopseudomonas viridis. Biochemistry **30:**1303–1310. http://dx.doi.org/10.1021/bi00219a021.
33. **Bose A, Newman DK.** 2011. Regulation of the phototrophic iron oxidation (pio) genes in Rhodopseudomonas palustris TIE-1 is mediated by the global regulator, FixK. Mol. Microbiol. **79:**63–75. http://dx.doi.org/10.1111/j.1365-2958.2010.07430.x.
34. **Moss DA, Leonhard M, Bauscher M, Mantele W.** 1991. Electrochemical redox titration of cofactors in the reaction center from Rhodobacter sphaeroides. FEBS Lett. **283:**33–36. http://dx.doi.org/10.1016/0014-5793(91)80547-G.
35. **Pereira MM, Antunes AM, Nunes OC, Da Costa MS, Teixeira M.** 1994. A membrane-bound HIPIP type center in the thermohalophile Rhodothermus marinus. FEBS Lett. **352:**327–330. http://dx.doi.org/10.1016/0014-5793(94)00985-6.
36. **Pereira MM, Carita JN, Teixeira M.** 1999. Membrane-bound electron transfer chain of the thermohalophilic bacterium Rhodothermus marinus: a novel multihemic cytochrome bc, a new complex III. Biochemistry **38:**1268–1275. http://dx.doi.org/10.1021/bi9818063.
37. **Brasseur G, Bruscella P, Bonnefoy V, Lemesle-Meunier D.** 2002. The bc(1) complex of the iron-grown acidophilic chemolithotrophic bacterium Acidithiobacillus ferrooxidans functions in the reverse but not in the forward direction. Is there a second bc(1) complex? Biochim. Biophys. Acta **1555:**37–43. http://dx.doi.org/10.1016/S0005-2728(02)00251-7.
38. **Bruscella P, Cassagnaud L, Ratouchniak J, Brasseur G, Lojou E, Amils R, Bonnefoy V.** 2005. The HiPIP from the acidophilic Acidithiobacillus ferrooxidans is correctly processed and translocated in Escherichia coli, in spite of the periplasm pH difference between these two micro-organisms. Microbiology **151**(Pt 5)**:**1421–1431. http://dx.doi.org/10.1099/mic.0.27476-0.
39. **Beinert H, Kiley PJ.** 1999. Fe-S proteins in sensing and regulatory functions. Curr. Opin. Chem. Biol. **3:**152–157. http://dx.doi.org/10.1016/S1367-5931(99)80027-1.